January 2013

Mouse strain-dependent variation in obesity and glucose homeostasis in response to high-fat feeding

M K. Montgomery
Garvan Institute Of Medical Research,University of Wollongong

N L. Hallahan
Garvan Institute Of Medical Research

S H. Brown
University of Wollongong, simonb@uow.edu.au

M Liu
Garvan Institute Of Medical Research

T W. Mitchell
University of Wollongong, toddm@uow.edu.au

See next page for additional authors

Mouse strain-dependent variation in obesity and glucose homeostasis in response to high-fat feeding

Abstract

Aims/hypothesis: Metabolic disorders are commonly investigated using knockout and transgenic mouse models. A variety of mouse strains have been used for this purpose. However, mouse strains can differ in their inherent propensities to develop metabolic disease, which may affect the experimental outcomes of metabolic studies. We have investigated strain-dependent differences in the susceptibility to diet-induced obesity and insulin resistance in five commonly used inbred mouse strains (C57BL/6J, 129X1/SvJ, BALB/c, DBA/2 and FVB/N). Methods: Mice were fed either a low-fat or a high-fat diet (HFD) for 8 weeks. Whole-body energy expenditure and body composition were then determined. Tissues were used to measure markers of mitochondrial metabolism, inflammation, oxidative stress and lipid accumulation. Results: BL6, 129X1, DBA/2 and FVB/N mice were all susceptible to varying degrees to HFD-induced obesity, glucose intolerance and insulin resistance, but BALB/c mice exhibited some protection from these detrimental effects. This protection could not be explained by differences in mitochondrial metabolism or oxidative stress in liver or muscle, or inflammation in adipose tissue. Interestingly, in contrast with the other strains, BALB/c mice did not accumulate excess lipid (triacylglycerols and diacylglycerols) in the liver; this is potentially related to lower fatty acid uptake rather than differences in lipogenesis or lipid oxidation. Conclusions/interpretation: Collectively, our findings indicate that most mouse strains develop metabolic defects on an HFD. However, there are inherent differences between strains, and thus the genetic background needs to be considered carefully in metabolic studies.

Keywords

strain, dependent, homeostasis, response, feeding, variation, fat, obesity, glucose, high, mouse

Disciplines

Medicine and Health Sciences

Publication Details

Montgomery, M. K., Hallahan, N. L., Brown, S. H., Liu, M., Mitchell, T. W., Cooney, G. J. & Turner, N. (2013). Mouse strain-dependent variation in obesity and glucose homeostasis in response to high-fat feeding. Diabetologia, 56 (5), 1129-1139.

Authors

M K. Montgomery, N L. Hallahan, S H. Brown, M Liu, T W. Mitchell, G J. Cooney, and N Turner

Mouse strain dependent variation in diet-induced obesity and insulin resistance

Running title: Genetic background and insulin resistance

Magdalene K. Montgomery[1], Nicole L. Hallahan[1], Simon Brown[2,3], Menghan Liu[1], Todd W. Mitchell[2,3], Gregory J. Cooney[1,4] & Nigel Turner[1,4*]

[1]Diabetes & Obesity Research Program, Garvan Institute of Medical Research, Darlinghurst, NSW, Australia; [2]School of Health Sciences, University of Wollongong, Wollongong, NSW, Australia; [3]Illawarra Health and Medical Research Institute, University of Wollongong, Wollongong, NSW, Australia; [4]St Vincent's Hospital Clinical School, University of New South Wales, Sydney, NSW, Australia

*Address correspondence to:

Nigel Turner, PhD
Diabetes & Obesity Research Program
Garvan Institute of Medical Research
384 Victoria St,
Darlinghurst, NSW,
Australia 2010

Phone: +61 2 9295 8236
Fax: +61 2 9295 8201
Email: n.turner@garvan.org.au

Words: 4400

Tables: 2

Figures: 6

Supplementary files: 1

Abstract

Metabolic disorders are commonly investigated using knockout and transgenic mouse models. A variety of mouse strains have been used for this purpose. However, mouse strains differ in their inherent propensities to develop metabolic disease, and this may affect the experimental outcomes of metabolic studies. We have investigated strain-dependent differences in the susceptibility to diet-induced obesity and insulin resistance in five commonly used mouse strains (C57BL/6J, 129X1/SvJ, BALB/c, DBA/2 and FVB/N). BL6, 129X1, DBA/2 and FVB/N mice were all susceptible to varying degrees to high-fat diet (HFD)-induced obesity, glucose intolerance and insulin resistance, but BALB/c exhibited some protection from the detrimental effects of a HFD. This protection could not be explained by differences in mitochondrial metabolism or oxidative stress in liver or muscle or inflammation in adipose tissue. Interestingly BALB/c mice were the only strain that did not accumulate excess lipid in the liver, which may be related to lower fatty acid uptake rather than differences in lipogenesis or lipid oxidation. Collectively, our findings indicate that aside from the BALB/c strain, the other mouse strains examined in this study are all suitable models for investigating metabolic defects induced by dietary lipid oversupply.

Introduction

In the past 30 years, the use of transgenic and knockout mouse strains to investigate the role of a specific protein in metabolic disease has become common place in medical research. However, when creating a genetically-manipulated mouse model, consideration must be given to the genetic background on which the mouse is created and the differences in metabolic phenotype that might be associated with investigating gene manipulation on mixed genetic backgrounds. Several previous studies have shown that mouse strains can differ substantially in their metabolic phenotype under normal low-fat diet conditions and in response to a high fat diet (1-3). Problems with these and other previous strain comparisons

are the use of diverse high-fat diets varying in lipid and carbohydrate content, the investigation of limited parameters that may underpin the development of metabolic disease and importantly some contradictory findings. For example, FVB/N mice have been previously characterized as obesity-prone (4) or obesity-resistant (3), and similar contradictory observations have been reported for DBA/2 mice (1; 5).

The C57BL/6 mouse strain is generally suggested to be the best strain for studying metabolic disease. However, it is worth noting that BL6 mice have also been described as "diabetes-prone" or "diabetes-resistant" depending on which other mouse strain was used in the comparison (6). The preference for the use of C57BL/6 mice probably stems from studies where it was shown that a high-fat and high-sucrose diet caused a 50% increase in fasting glucose and a 10-fold increase in plasma insulin levels (7), demonstrating obesity-induced insulin resistance in this particular strain. The susceptibility of C57BL/6 mice to develop glucose intolerance was later shown to be to some extent due to impaired insulin secretion (8; 9). Because of the utility of using 129X1/SvJ mouse embryonic stem cells for the generation of gene manipulated strains, much of the original metabolic phenotyping in knockout and transgenic mice was performed using mice produced on this strain or more frequently using mice backcrossed to C57BL/6 for a defined or undefined number of generations (10). There is however clear evidence that genetically manipulated mice on a mixed 129/BL6 can display different phenotype to mice where the same genetic manipulation is performed on a pure genetic background (11).

A number of mechanisms have been proposed to be responsible for obesity-related insulin resistance, lipid accumulation in non-adipose tissues, inflammation in adipose and other tissues, mitochondrial dysfunction, and/or oxidative stress. Much of the evidence supporting these various theories is based on studies in normal or genetically manipulated mice fed high-fat diets, however it is still not completely resolved to what extent these factors

may be related to the genetic background of mice. Here, we report studies on the response of five commonly used mouse strains (C57BL/6, 129X1/SvJ, BALB/c, DBA/2 and FVB/N) to the same high-fat diet, examining glucose tolerance, whole-body and tissue-specific lipid accumulation, and aspects of tissue inflammation, mitochondrial function and oxidative stress.

Research design and methods

Eight-week old C57BL/6J, 129X1/SvJ, BALB/c, DBA/2 and FVB/N mice were purchased from the Australian Resource Centre (Perth, Australia). Mice were housed with 4 animals per cage in a temperature-controlled room (22°C ± 1°C) with a 12-hour light/dark cycle and ad libitum access to food and water. After one week on a standard low-fat laboratory diet (low fat; 8% calories from fat, 21% calories from protein, 71% calories from carbohydrate; Gordon's Specialty Stock Feeds, Yanderra, NSW, Australia), mice from each strain were randomly allocated to remain on the low-fat diet (LFD) or to receive a high-fat diet (HFD) *ad libitum* for 8 weeks. The HFD was made in-house (12) and is based on rodent diet no. D12451 (containing 45% of calories from lard) (Research Diets, New Brunswick, NJ). During the 8-week feeding period, body weight and food intake was monitored on a bi-weekly basis. As all mice were kept in cages of 4 animals, food intake per cage was averaged and is expressed in kJ/mouse/day. All experiments were carried out with the approval of the Garvan Institute/St. Vincent's Hospital Animal Experimentation Ethics Committee, following guidelines issued by the National Health and Medical Research Council of Australia.

Determination of body composition and energy expenditure.

Fat and lean body mass were measured in mice using dual-energy X-ray absorptiometry (DXA) (Lunar PIXImus2 mouse densitometer; GE Healthcare) in accordance with the manufacturer's instructions. Oxygen consumption rate (VO_2) and respiratory control ratio

(RER) of individual mice was measured using an eight-chamber indirect calorimeter (Oxymax series; Columbus Instruments, Columbus, OH) as previously described (13).

In vivo glucose tolerance.

Mice were fasted for 6 hours (from 8am) and then injected intraperitoneally with glucose (2 g/kg) or insulin (0.75 U/kg), and blood glucose levels were monitored over time using an Accu-check II glucometer (Roche Diagnostics, Castle Hill, Australia). During the glucose tolerance test some samples were collected for plasma insulin determination by radioimmunoassay using a rat-specific kit (Linco Research, St. Charles, MO).

Palmitate oxidation.

Palmitate oxidation was measured in muscle and liver homogenates as described previously (13). CO_2 produced during the incubation was collected in 100 µl of 1 M sodium hydroxide. ^{14}C counts present in the acid-soluble fraction were also measured and combined with the CO_2 values to give the total palmitate oxidation rate. Protein content in the homogenates was measured using the Bradford method (protein assay kit; Bio-Rad Laboratories, Regents Park, Australia).

Tissue lipid analyses.

Lipids were extracted from tissues by standard methods (14). Plasma, muscle and liver triglyceride contents were determined using a colorimetric assay kit (Triglycerides GPO-PAP; Roche Diagnostics, Indianapolis, IN) as previously described (15). Similarly, plasma NEFAs were measured using a colorimetric kit (WAKO diagnostics, Osaka, Japan). Full details of the methods for diacyglycerol (DAG) and ceramide measurements can be found in the Supplementary file. Briefly, lipids were extracted from muscle and liver in solvents

containing 2 nmoles of ceramide (17:0) and 10 nmoles of DAG (17:0/17:0). DAG and ceramide levels were measured using a hybrid linear ion trap-triple quadrupole mass spectrometer (QTRAP® 5500, ABSCIEX, Foster City, CA, USA) and data were analyzed with LipidView® (ABSCIEX) version 1.1.

SDS-PAGE and immunoblotting.

Whole-tissue lysates were prepared from powdered muscle and liver by manual homogenization in RIPA buffer (16) followed by incubation for 2 hours at 4 °C and centrifugation for 10 min at 12,000 *g*. Protein content of supernatants was quantified using the Bradford method. 20 μg of protein were denatured in Laemmli buffer for 15min at 65 °C and then resolved by SDS-PAGE electrophoresis (Invitrogen). Protein was electrotransferred onto polyvinylidine difluoride membranes, immunoblotted and quantitated, as described previously (17). Detailed information on immunoblotting can be found in the Supplementary file.

Enzyme activity measurements.

Muscle and liver samples were manually homogenized 1:8 (wt/vol) in 50 mM Tris-HCl, 1 mM EDTA and 0.1% Triton X-100, pH 7.2, followed by centrifugation for 10 min at 5,000 g. Supernatants were used to determine citrate synthase (CS) and β-hydroxyacyl CoA dehydrogenase (βHAD) activity at 30 °C as described previously (13) using a temperature-controlled spectrophotometer (Spectra Max 250, Molecular Devices, Sunnyvale, CA). Glutathione peroxidase (GPx) activity was determined as the decrease in NADPH absorption at 340 nm and 30 °C, as described previously (18).

Gene expression analysis.

RNA was extracted using TRI-Reagent (Sigma-Aldrich) according to the manufacturer's protocol, followed by DNAse treatment (RQ1 RNase-free DNase, Promega) and synthesis of complementary DNA using Random primer 9 (New England Biolabs) and Superscript III reverse transcriptase (Invitrogen) according to the manufacturer's instructions. Real-time PCR was performed using the Lightcycler® 480 Probes Master mix on a real-time PCR System (7900HT; Applied Biosystems). The value obtained for each specific product was normalised to a control gene (Hypoxanthine-guanine phosphoribosyltransferase) and the results are expressed as fold-change of the HFD-fed mice vs. the LFD-fed mice for each strain. Primer sequences are shown in Supplementary Table 1.

Oxidative damage biomarkers.

Muscle and liver samples were homogenized as described above for the enzyme activity measures. TBARS were determined, as described previously (19). For the determination of protein carbonylation, nucleic acids were removed using 1% streptomycin (incubation at room temperature for 15 min, followed by centrifugation at 6000 g, 10 min, 4 °C) (20), and the supernatant used for the assay. Protein carbonyls were derivatized to 2,4-dinitrophenylhydrazone by reaction with 2,4-dinitrophenylhydrazine (DNPH) as described previously (21). Lipid hydroperoxides (LOOH) were measured using the FOX2-Assay, as described previously (22).

Statistical analysis

Data analysis was performed using JMP 5.1 (Statistical Analysis System Institute Inc., Cary, NC, USA). All results are given as mean ± standard error with n being the number of animals used in each assay and $P = 0.05$ set as the level of significance. Data were tested for

normality using the Shapiro–Wilk W test and homogeneity of variance using the O'Brien and Brown-Forsythe tests. Data not normally distributed were compared using non-parametric Wilcoxon/Kruskal–Wallis tests and any data showing unequal variance were compared using a Welch ANOVA. For each mouse strain, a one-way ANOVA was completed with low-fat or high-fat diet as the independent variable and the measured metabolic parameters as dependent variables. Means were then compared using the Tukey–Kramer honestly significant difference test.

Results

Body weight, fat mass and food intake during high-fat feeding

Compared to animals remaining on a LF diet, body weight was significantly increased in Bl6, 129X1, DBA/2 and FVB/N mice fed the high-fat, but remained unchanged in BALB/c mice. High-fat fed DBA/2 and 129X1 mice showed the largest increase in body weight in comparison to all other strains (25 % increase for both strains) (Fig. 1A). Whole-body adiposity measured by dual-energy X-ray absorptiometry was increased in all five mouse strains on the HFD, including the BALB/c mice, as was the size of the epididymal and inguinal fat depots (Table 1).

Food intake was measured bi-weekly as an average of 2 cages with 4 animals per cage for each mouse strain. The energy intake (shown in kJ/day) during the 8-week feeding period was higher in HFD-fed 129X1 and DBA/2 mice compared to LF controls, but was not significantly different in BL6, BALB/c and FVB/N mice (Table 1).

Whole-animal respiration and fuel selection, as well as tissue-specific lipid oxidation

Whole-animal oxygen consumption, corrected for lean mass (as determined by DXA), was significantly increased to a similar extent in all mouse strains on the HFD (11-16% increase).

Similarly, the respiratory exchange ratio (RER) was significantly decreased in all five strains consistent with increased lipid intake and catabolism (Table 1).

Glucose tolerance and insulin sensitivity

To determine the effect of HFD on whole-body glucose metabolism, we examined glucose clearance during an intraperitoneal glucose tolerance test (ipGTT) (Fig. 1B). In four of the mouse strains, the HFD-fed animals displayed a significant impairment in glucose tolerance, demonstrated by a substantial increase in the incremental glucose area under the curve (AUC) (BL6 +97%, 129X1 +284%, DBA/2: +130%, FVB/N +37%). In contrast, BALB/c mice exhibited no deterioration in glucose tolerance on the HFD, (AUC: -0.6% vs. LFD).

To examine the insulin response to elevated blood glucose levels, we measured insulin levels during the ipGTT (Suppl. Fig. 1). Despite all five mouse strains (particularly DBA/2) having higher insulin levels during the ipGTT when on the HFD in comparison to their LFD-counterparts, BALB/c mice on the HFD had the lowest plasma insulin levels for all time points during the GTT in comparison to all other HFD-fed mouse strains (see Table 2 for fasting insulin = zero time point during GTT). Similarly, fasting blood glucose and fasting plasma insulin were significantly increased in all mouse strains on the HFD except for BALB/c (Table 2). As an indicator of insulin sensitivity, 'fasting glucose' was multiplied by 'fasting insulin' and is presented as an Insulin Sensitivity Index (ISI) for each diet group and mouse strain. The ISI demonstrated substantial impairment in insulin sensitivity in all mouse strains, except the BALB/c (increase in ISI value vs. LFD group: BL6 +96%, 129X1 +128%, BALB/c: +4%, DBA/2: +234%, FVB/N +70%). An intraperitoneal insulin tolerance test (ipITT) was used as a second measure of insulin sensitivity (Suppl. Fig. 2). Similarly to the ISI, the AUC for the ipITT indicated the development of insulin resistance in all high-fat fed

mouse strains, except BALB/c (increase in AUC values vs. LFD group: BL6 +22%, 129X1 +16%, BALB/c: -8%, DBA/2: +56%, FVB/N +39%).

Lipid accumulation in non-adipose tissues

Due to the well-established link between insulin resistance and intracellular lipid accumulation in non-adipose tissues (23), we examined lipid accumulation in quadriceps muscle and liver of all LF- and HF-fed mice. All HF-fed mouse strains showed an increased triglyceride deposition in their muscles, while only the FVB/N strain also displayed elevated DAG and ceramide content (Fig 2). In the liver, triglyceride and DAG levels were significantly increased in BL6, 129X1, DBA/2 and FVB/N mice, with a decreased ceramide level also observed in liver from BL6 mice. Intriguingly, HF-fed BALB/c mice did not accumulate any excess triglyceride or DAG in their livers compared to LF controls, and also displayed a 25% reduction in ceramide levels (Fig. 2).

Markers of mitochondrial oxidative metabolism in liver and skeletal muscle

Causative links have been proposed between mitochondrial dysfunction and intracellular lipid accumulation and insulin resistance (24). To determine if insulin resistance and lipid accumulation in BL6, 129X1, DBA/2 and FVB/N mice on the HFD was accompanied by differences in mitochondrial fuel utilization, and to identify if the absence of lipid accumulation in BALB/c liver was due to an increase in mitochondrial oxidation, we have examined several markers of mitochondrial metabolism.

Figures 3 and 4 show representative immunoblotting analysis of a variety of markers of mitochondrial metabolism. In skeletal muscle, there was a significant increase in PGC1α, UCP3, PDK4 and sub-units of the complexes of the electron transport chain (ETC) in all mouse strains on the HFD, except the BALB/c (for details in percentage changes refer to Fig. 3A). In BALB/c muscle, mitochondrial proteins were either unchanged or decreased in the

HFD-fed animals. A similar trend was observed with citrate synthase (CS) and β-hydroxyacyl CoA dehydrogenase (βHAD) activity in skeletal muscle, with BALB/c being the only strain that showed no increase in these enzyme activities on the HFD (Fig. 3B and 3C). Furthermore, to determine the effect of HFD on fatty acid oxidative capacity, we measured the rate of palmitate oxidation in muscle and liver. Skeletal muscle from fat-fed mice from all mouse strains, including the BALB/c mice, displayed an increased capacity for palmitate oxidation (Suppl. Fig. 4). Although there was a slight increase in fatty acid oxidation in BALB/c muscle, the collective findings suggest, that a HFD in Bl6, 129X1, DBA/2 and FVB/N mice leads to stimulation of mitochondrial oxidative pathways, whereas BALB/c mice show little change in the same skeletal muscle parameters in response to the HFD.

In the liver, CS and βHAD enzymatic activity was significantly increased in 129X1, DBA/2 and FVB/N mice, but not in BL6 and BALB/c mice (Suppl. Fig. 3). Western blot analysis in the liver showed a significant increase in PGC1α, CPT1 and complex II of the ETC in high-fat fed BL6 mice, a decrease in a variety of mitochondrial markers in FVB/N mice, and no change in any other strain (Fig. 4). Furthermore, the palmitate oxidation rate, used as a marker of fatty acid oxidative capacity of the liver, was unchanged on the HFD in all mouse strains (Suppl. Fig. 4). These findings suggest that the absence of lipid accumulation in liver of HFD BALB/c mice is not due to an increase in mitochondrial lipid utilization.

Lipid synthesis and uptake in the liver

Because BALB/c mice did not accumulate liver lipid on a HFD and did not exhibit increased mitochondrial oxidative capacity, we examined the protein expression of several markers of lipogenesis and fatty acid uptake into the liver. The protein expression of FAS, ACC and SCD-1 was decreased in all strains except the DBA/2 which showed unchanged FAS and SCD-1 levels and an increased ACC protein expression on the HFD (Fig. 4). High-fat fed

BALB/c mice showed a similar reduction in lipogenesis as other mouse strains, suggesting that a decrease in lipogenic capacity could not explain the lower liver lipid content in BALB/c mice.

Furthermore, we measured protein expression of the major hepatic fatty acid transport proteins (FATP) 2 and 4 as markers of fatty acid uptake into the liver. High-fat fed BALB/c and BL6 mice were the only strains that did not show a consistent increase in liver fatty acid transport proteins in comparison to their LFD-counterparts. In fat-fed BALB/c mice, protein expression of FATP2 remained unchanged, whereas FATP4 was even lower compared to the LFD-fed mice (Fig. 4). These results suggest that lipid accumulation in BALB/c liver on a HFD might be limited by a reduced capacity for fatty acid uptake.

Diet-induced changes in inflammation in adipose tissue and liver

The reduced insulin action associated with diet-induced obesity has been frequently linked to increased inflammation in adipose and other tissues. To determine if differences in glucose tolerance and insulin resistance in the mouse strains was associated with macrophage infiltration in adipose tissue, we examined the gene expression of F4/80, CD68 and $CD11c^{+}$, which are surface markers of M1- and M2-macrophages, as well as TNFα, MCP-1 and IL-6 as markers of cytokine production by macrophages and adipocytes. F4/80, CD68 and $CD11c^{+}$ increased in adipose tissue of all HFD-fed mouse strains (Fig. 5), indicating that leukocyte and macrophage infiltration into adipose tissue is already present after 8 weeks of high-fat feeding in all mouse strains including BALB/c mice (Fig. 5 A-C). Interestingly, increased TNFα, MCP-1 and IL-6 mRNA levels were only present in BALB/c, DBA/2 and FVB/N mice, demonstrating that not all strains respond to increased macrophage infiltration with increased cytokine expression after 8 weeks on the HFD (Fig. 5 D-F). Together, the gene expression analysis does not support adipose tissue inflammation as a major reason for the

different glucose handling observed in HFD-fed BALB/c mice. In addition, we have measured protein expression of JNK, IKKα and IKKβ, IκB (total and phosphorylated for all except IκB) as markers of liver inflammation in the liver of LFD- and HFD mice and found no changes in any liver inflammation marker after 8 weeks of high-fat feeding (data not shown).

Diet-induced oxidative stress: Antioxidant protection & Oxidative damage

To determine if lipid accumulation in muscle and liver correlates with oxidative damage to lipids and to examine if lower oxidative stress levels could partly explain the differences observed in BALB/c mice, we measured lipid hydroperoxides (LOOH) and TBARS (thiobarbituric acid reactive substances) in those two tissues. In muscle, LOOH and TBARS levels were significantly decreased in BALB/c mice on the HFD whereas there was a trend to increased oxidative damage in the other strains. (Fig. 6 A+B). In the liver however, HFD BALB/c mice were the only strain that displayed increased lip-oxidative damage compared to LFD-counterparts (Fig. 6 C+D). In addition to lower LOOH and TBARS levels in muscle of HFD BALB/c mice, protein carbonylation and glutathione peroxidase (GPx) activity were also significantly decreased (Suppl. Fig. 5), suggesting decreased oxidative stress in muscle of HFD BALB/c mice, but not in the other mouse strains. Low oxidative stress in skeletal muscle, but not in the liver, might be one of the mechanisms responsible to the lack of glucose intolerance and insulin resistance observed in BALB/c mice fed the HFD.

Discussion

The data obtained in this study gives a clear indication of the similarities and differences in a number of metabolic parameters in five commonly used mouse strains in response to eight weeks of feeding with a HFD. On a HFD all strains of mice gained a significant amount of body fat. All strains except BALB/c also exhibited a significant but variable deterioration in

glucose tolerance. Intriguingly BALB/c mice maintained normal glucose tolerance despite increased adiposity, increased muscle triglyceride accumulation, oxidative stress in liver and elevated levels of adipose tissue inflammation. This is somewhat surprising because increases in all these parameters have previously been suggested to be key abnormalities predisposing to insulin resistance and increasing the risk of developing type 2 Diabetes. The most obvious difference in BALB/c mice that might explain their ability to maintain glucose tolerance on a HFD was the lack of lipid accumulation in liver in this strain. All other strains had significant accumulation of triglycerides and DAGs in liver on the HFD and significant glucose intolerance.

Lipid accumulation in non-adipose tissues has been shown to be closely related to the development of glucose intolerance and insulin resistance (23; 25). In the current study BALB/c mice displayed a similar pattern of lipid accumulation in muscle to the other four mouse strains. This suggests that in the current investigation muscle lipid accumulation was not a major determinant of glucose tolerance across the different strains. Intriguingly, fat-fed BALB/c mice did display a disparate lipid profile to the other strains in the liver, with no excess triglyceride or DAG accumulation and a reduced ceramide content. This difference in liver lipid accumulation may partly explain the maintained glucose tolerance and insulin action in the BALB/c mice fed a HFD and is potentially due to lower rates of fatty acid uptake in BALB/c liver. In BALB/c, the expression of FATP2 and FATP4, which are the most abundant fatty acid transporters expressed in the liver (26), remained either unchanged (FATP2) or was decreased (FATP4) whereas in most other strains the amount of these transporters increased when fed a HFD. The BALB/c mice phenotype of increased fat mass but normal glucose tolerance seems similar to the recently described metabolically healthy obese (MHO) humans. MHO humans, despite having severe adiposity, remain relatively insulin sensitive, as indicated by HOMA-IR and euglycaemic-hyperinsulinemic clamps (27).

Interestingly, one of the observed metabolic differences between MHO and obese insulin-resistant humans was liver lipid content, with the metabolically-healthy obese individuals displaying low liver lipid accumulation, despite visceral adiposity (28). Obesity in BALB/c mice might well provide an opportunity to further investigate the links between lipid metabolism in liver and glucose tolerance.

Each of the five mouse strains examined exhibited defined but different physiological responses to a high-fat diet. This difference in metabolic response was clearly apparent when comparing the GTT curves. Although HFD-fed BL6, 129X1, DBA2 and FVB/N mice all became glucose intolerant, the response of each strain to a glucose bolus differed substantially, both on low-fat and high-fat diets. For example, FVB/N mice on a standard LFD are relatively glucose intolerant in comparison to the other strains, and have similar glucose tolerance to BL6 mice on a HFD. BL6 mice are the most common mouse strain used in the study of metabolic disease, as they have been suggested to be the most susceptible to the development of diet-induced obesity and insulin resistance. In the present investigation BL6 mice displayed intermediate adiposity, insulin resistance and lipid accumulation in muscle and liver when compared to the other four mouse strains investigated. The strain that accumulated the most fat (37% of total body weight) and exhibited the greatest glucose intolerance on a HFD (3-fold increase in AUC) was the 129X1 strain. A large number of genetically manipulated mice are produced on the 129X1 background and then backcrossed to BL6 for varying generations. The clear difference in glucose tolerance and other metabolic parameters between BL6 and 129X1 suggest it is extremely important to know the extent of a mixed background in genetically manipulated mice before drawing conclusions about the influence of a specific gene on metabolic homeostasis.

DBA/2 mice also displayed an interesting response to a high-fat diet. Although DBA/2 show the largest increase in body weight and also gained substantial amounts of fat mass, they

become only marginally glucose intolerant on the HFD. DBA/2 exhibited similar differences in lipid accumulation, mitochondrial metabolism, inflammation and oxidative stress to other strains, however, DBA/2 mice did exhibit a large increase in fasting insulin, and the largest excursion of plasma insulin levels during the glucose tolerance test, suggesting that it is compensatory hyperinsulinemia that reduces HFD-induced glucose intolerance in this strain (1; 8).

Mitochondrial dysfunction, oxidative stress and inflammation are commonly suggested as mediators of insulin resistance and glucose intolerance in obese animal models and obese humans (23; 24). In the current study all the of the mouse strains (except BALB/c) responded to a HFD as BL6 mice did in our previous study, with a modest increase in the expression, as well as activity of mitochondrial proteins, and an increase in capacity to oxidize fatty acids (13). BALB/c mice were the only mouse strain where mitochondrial oxidative capacity remained unchanged (enzyme activities) or was even decreased (protein expression) in high-fat fed animals and glucose tolerance was preserved in this strain. These results suggest the HFD-induced changes in muscle mitochondrial capacity do not correlate with glucose tolerance in these mouse strains. Oxidative stress in liver and muscle of all strains was also assessed by examining levels of lipid hydroperoxides and TBARS. The only consistent effect was that HFD increased markers of lipid peroxidation in liver of BALB/c mice, but decreased these markers in muscle of the same animals, which again is difficult to reconcile against the observation that BALB/c mice maintain normal glucose tolerance and insulin action on a HFD. Investigation of the inflammatory state of adipose tissue in the different strains of HFD-fed mice, produced substantial evidence of macrophage infiltration (increased F4/80 and CD11c gene expression) in all strains and evidence of increased cytokine expression (TNF and MCP-1) in 3 of the 5 strains including BALB/c. These results demonstrate that adipose tissue inflammation can be observed within 8 weeks of a HFD, even in the presence

of normal glucose tolerance and insulin action in BALB/c mice, and thus support the notion that inflammation may only contribute to glucose tolerance and insulin action after long-term high fat feeding (29; 30).

Altogether, this extensive comparison of the effects of a HFD on different mouse strains demonstrates that all strains accumulate body fat and show signs of adipose tissue inflammation and muscle lipid accumulation. However, the effect of fat accumulation on markers of glucose homeostasis is variable and strain dependent. In particular, BALB/c mice remain glucose tolerant on a HFD and this seems directly related to the lack of accumulation of fat in liver of these mice, despite lipid accumulation in muscle. The results suggest that liver lipid content is a major determinant of glucose tolerance and also highlight the need for caution when comparing results of dietary interventions in studies involving different or mixed strains of mice.

Acknowledgements

This work was supported by grants from the National Health and Medical Research Council of Australia (NHMRC). No potential conflicts of interest relevant to this article were reported.

References

1. Andrikopoulos S, Massa CM, Aston-Mourney K, Funkat A, Fam BC, Hull RL, Kahn SE, Proietto J: Differential effect of inbred mouse strain (C57BL/6, DBA/2, 129T2) on insulin secretory function in response to a high fat diet. Journal of Endocrinology 187:45-53, 2005
2. Berglund ED, Li CY, Poffenberger G, Ayala JE, Fueger PT, Willis SE, Jewell MM, Powers AC, Wasserman DH: Glucose metabolism in vivo in four commonly used inbred mouse strains. Diabetes 57:1790-1799, 2008
3. Boudina S, Sena S, Sloan C, Tebbi A, Han YH, O'Neill BT, Cooksey RC, Jones D, Holland WL, McClain DA, Abel ED: Early Mitochondrial Adaptations in Skeletal Muscle to Diet-Induced Obesity Are Strain Dependent and Determine Oxidative Stress and Energy Expenditure But Not Insulin Sensitivity. Endocrinology 153:2677-2688, 2012
4. Metlakunta AS, Sahu M, Sahu A: Hypothalamic phosphatidylinositol 3-kinase pathway of leptin signaling is impaired during the development of diet-induced obesity in FVB/N mice. Endocrinology 149:1121-1128, 2008
5. Fearnside JF, Dumas ME, Rothwell AR, Wilder SP, Cloarec O, Toye A, Blancher C, Holmes E, Tatoud R, Barton RH, Scott J, Nicholson JK, Gauguier D: Phylometabonomic Patterns of Adaptation to High Fat Diet Feeding in Inbred Mice. Plos One 3, 2008
6. Clee SM, Attie AD: The genetic landscape of type 2 diabetes in mice. Endocr Rev 28:48-83, 2007
7. Surwit RS, Feinglos MN, Rodin J, Sutherland A, Petro AE, Opara EC, Kuhn CM, Rebuffescrive M: Differential effects of fat and sucrose on the development of obesity and diabetes in C57BL/6J and A/J mice. . Metabolism-Clinical and Experimental 44:645-651, 1995
8. Goren HJ, Kulkarni RN, Kahn CR: Glucose homeostasis and tissue transcript content of insulin signaling intermediates in four inbred strains of mice: C57BL/6, C57BLKS/6, DBA/2, and 129X1. Endocrinology 145:3307-3323, 2004
9. Toye AA, Lippiat JD, Proks P, Shimomura K, Bentley L, Hugill A, Mijat V, Goldsworthy M, Moir L, Haynes A, Quarterman J, Freeman HC, Ashcroft FM, Cox RD: A genetic and physiological study of impaired glucose homeostasis control in C57BL/6J mice. Diabetologia 48:675-686, 2005
10. Wolfer DP, Crusio WE, Lipp HP: Knockout mice: simple solutions to the problems of genetic background and flanking genes. Trends in Neurosciences 25:336-340, 2002
11. Pi J, Bai Y, Daniel KW, Liu D, Lyght O, Edelstein D, Brownlee M, Corkey BE, Collins S: Persistent Oxidative Stress Due to Absence of Uncoupling Protein 2 Associated with Impaired Pancreatic Î²-Cell Function. Endocrinology 150:3040-3048, 2009
12. Sainsbury A, Bergen HT, Boey D, Bamming D, Cooney GJ, Lin S, Couzens M, Stroth N, Lee NJ, Lindner D, Singewald N, Karl T, Dury L, Enriquez R, Slack K, Sperk G, Herzog H: Y2Y4 receptor double knockout protects against obesity due to a high-fat diet or Y1 receptor deficiency in mice. Diabetes 55:19-26, 2006
13. Turner N, Bruce CR, Beale SM, Hoehn KL, So T, Rolph MS, Cooney GJ: Excess lipid availability increases mitochondrial fatty acid oxidative capacity in muscle: evidence against a role for reduced fatty acid oxidation in lipid-induced insulin resistance in rodents. Diabetes 56:2085-2092, 2007
14. Folch J, Lees M, Stanley GHS: A simple method for the isolation and purification of total lipids from animal tissues. Journal of Biological Chemistry 226:497-509, 1957
15. Ye JM, Iglesias MA, Watson DG, Ellis B, Wood L, Jensen PB, Sorensen RV, Larsen PJ, Cooney GJ, Wassermann K, Kraegen EW: PPARalpha /gamma ragaglitazar eliminates fatty liver and enhances insulin action in fat-fed rats in the absence of hepatomegaly. Am J Physiol Endocrinol Metab 284:E531-540, 2003
16. Cleasby ME, Lau Q, Polkinghorne E, Patel SA, Leslie SJ, Turner N, Cooney GJ, Xu A, Kraegen EW: The adaptor protein APPL1 increases glycogen accumulation in rat skeletal muscle through activation of the PI3-kinase signalling pathway. Journal of Endocrinology 210:81-92, 2011
17. Cleasby ME, Dzamko N, Hegarty BD, Cooney GJ, Kraegen EW, Ye JM: Metformin prevents the development of acute lipid-induced insulin resistance in the rat through altered hepatic signaling mechanisms. Diabetes 53:3258-3266, 2004

18. Montgomery MK, Buttemer WA, Hulbert AJ: Does the oxidative stress theory of aging explain longevity differences in birds? II. Antioxidant systems and oxidative damage. Experimental Gerontology 47:211-222, 2012
19. Buege SD, Aust SD: Microsomal lipid peroxidation. Methods Enzymol. 52:302–310, 1978
20. Pamplona R, Prat J, Cadenas S, Rojas C, PerezCampo R, Torres M, Barja G: Low fatty acid unsaturation protects against lipid peroxidation in liver mitochondria from long-lived species: The pigeon and human case. Mechanisms of Ageing and Development 86:53-66, 1996
21. Levine RL, Garland D, Oliver CN, Amici A, Climent I, Lenz AG, Ahn BW, Shaltiel S, Stadtman ER: Determination of carbonyl content in oxidatively modified proteins. Methods Enzymol 186:464-478, 1990
22. Bou R, Codony R, Tres A, Decker EA, Guardicila F: Determination of hydroperoxides in foods and biological samples by the ferrous oxidation-xylenol orange method: A review of the factors that influence the method's performance. Analytical Biochemistry 377:1-15, 2008
23. Samuel VT, Shulman GI: Mechanisms for Insulin Resistance: Common Threads and Missing Links. Cell 148:852-871, 2012
24. Turner N, Heilbronn LK: Is mitochondrial dysfunction a cause of insulin resistance? Trends in Endocrinology and Metabolism 19:324-330, 2008
25. Kraegen EW, Cooney GJ: Free fatty acids and skeletal muscle insulin resistance. Curr Opin Lipidol 19:235-241, 2008
26. Glatz JFC, Luiken J, Bonen A: Membrane Fatty Acid Transporters as Regulators of Lipid Metabolism: Implications for Metabolic Disease. Physiological Reviews 90:367-417, 2010
27. Samocha-Bonet D, Chisholm DJ, Tonks K, Campbell LV, Greenfield JR: Insulin-sensitive obesity in humans - a 'favorable fat' phenotype? Trends in Endocrinology and Metabolism 23:116-124, 2012
28. Stefan N, Kantartzis K, Machann J, Schick F, Thamer C, Rittig K, Balletshofer B, Machicao F, Fritsche A, Haring HU: Identification and characterization of metabolically benign obesity in humans. Archives of Internal Medicine 168:1609-1616, 2008
29. Lee YS, Li PP, Huh JY, Hwang IJ, Lu M, Kim JI, Ham M, Talukdar S, Chen A, Lu WJ, Bandyopadhyay GK, Schwendener R, Olefsky J, Kim JB: Inflammation Is Necessary for Long-Term but Not Short-Term High-Fat Diet Induced Insulin Resistance. Diabetes 60:2474-2483, 2011
30. Strissel KJ, DeFuria J, Shaul ME, Bennett G, Greenberg AS, Obin MS: T-Cell Recruitment and Th1 Polarization in Adipose Tissue During Diet-Induced Obesity in C57BL/6 Mice. Obesity 18:1918-1925, 2010

Tables

Table 1: Animal characteristics, including tissue weights, food intake and whole-animal respiration, separated by mouse strain and diet group

		C57Bl/6	129X1	BALB/c	DBA/2	FVB/N
Body weight	LFD	30.3±0.4	27.6±0.4	26.0±0.6	31.2±0.7	31.1±0.5
(g)	HFD	35.4±0.9 ‡	34.7±0.6 ‡	27.8±0.5	39.0±0.8 ‡	34.5±0.6 ‡
Fat mass	LFD	15.6±1.1	22.2±1.9	20.6±0.4	23.7±0.8	18.3±1.2
(%)	HFD	29.4±1.3 ‡	36.6±2.7 ‡	29.2±1.3 ‡	38.8±1.8 ‡	30.0±1.4 ‡
Tissue weights (g)						
eWAT	LFD	0.34±0.02	0.33±0.01	0.54±0.02	0.79±0.07	0.39±0.06
	HFD	1.42±0.15 ‡	1.38±0.05 ‡	1.09±0.10 ‡	1.82±0.10 ‡	1.17±0.06 ‡
iWAT	LFD	0.24±0.01	0.34±0.04	0.36±0.04	0.56±0.06	0.33±0.03
	HFD	0.74±0.14 ‡	0.94±0.07 ‡	0.54±0.03 †	1.55±0.11 ‡	0.63±0.03 ‡
BAT	LFD	0.12±0.01	0.12±0.01	0.15±0.03	0.17±0.01	0.17±0.02
	HFD	0.13±0.01	0.21±0.02 †	0.15±0.01	0.34±0.04 ‡	0.23±0.01 †
Liver	LFD	1.48±0.07	1.20±0.02	1.31±0.05	1.63±0.05	1.70±0.04
	HFD	1.21±0.08	1.25±0.07	1.17±0.02 *	1.64±0.04	1.71±0.04
Food Intake						
(kcal/day)	LFD	13.73±0.55	11.31±0.01	12.82±1.18	11.26±0.57	13.69±2.50
	HFD	14.17±1.20	18.00±2.71 *	12.89±0.23	16.10±2.28 *	13.65±0.50
Whole-body respiration						
(ml O_2/g/h)	LFD	4.27±0.08	4.46±0.15	4.71±0.10	4.63±0.09	4.19±0.10
	HFD	4.86±0.13 †	5.14±0.12 †	5.23±0.09 †	5.16±0.17 *	4.88±0.17 †
RER	LFD	0.97±0.03	0.94±0.01	0.97±0.02	0.88±0.02	0.95±0.01
	HFD	0.84±0.01 †	0.87±0.01 *	0.86±0.03 ‡	0.83±0.01	0.84±0.02 ‡

LFD vs. HFD: * $p<0.05$, † $p<0.01$ and ‡ $p<0.001$, n=6-8 for each strain and diet group; whole-animal oxygen consumption is corrected for lean mass; BAT = brown adipose tissue; eWAT = epididymal white adipose tissue; HFD = high-fat diet; iWAT = inguinal white adipose tissue; LFD = low-fat diet; RER = respiratory exchange ratio

Table 2: Plasma characteristics

		C57Bl/6	129X1	BALB/c	DBA/2	FVB/N
Glucose	LFD	9.14±0.36	6.59±0.28	7.96±0.34	8.21±0.36	9.67±0.36
(mM)	HFD	10.51±0.29†	7.31±0.25	7.74±0.16	9.90±0.50*	10.95±0.43*
Insulin	LFD	0.72±0.04	0.54±0.05	0.63±0.06	1.32±0.11	0.90±0.05
(ng/ml)	HFD	1.26±0.14†	1.08±0.09‡	0.64±0.05	2.41±0.32†	1.19±0.08*
Adiponectin	LFD	3.84±0.36	4.17±0.36	3.99±0.47	10.24±1.00	7.59±1.02
(µg/ml)	HFD	3.59±0.50	4.62±0.48	3.97±0.35	9.45±0.54	7.48±0.42
TAG	LFD	4.39±0.34	5.84±0.17	6.13±0.44	10.76±0.82	10.14±0.92
(µmol/ml)	HFD	4.52±0.27	7.22±0.40†	6.82±0.42	13.20±1.03	6.57±0.70*
NEFA	LFD	0.76±0.05	0.87±0.05	0.79±0.05	0.97±0.10	0.71±0.04
(µmol/ml)	HFD	0.79±0.02	0.85±0.08	0.85±0.06	1.01±0.08	0.66±0.04

LFD vs. HFD: * when $p<0.05$, † when $p<0.01$ and ‡ when $p<0.001$, n=8 for each strain and diet group; HFD = high-fat diet; LFD = low-fat diet; NEFA = non-esterified fatty acids; TAG = triglycerides

Figure legends

Figure 1: Body weight during the 8-week feeding period (A) and intraperitoneal glucose tolerance test (B) in low-fat (LF) and high-fat (HF) fed mice. Glucose (2g/kg) was injected at the 0 time point and blood glucose levels were monitored for 90min post-injection. black dots = LF mice, white dots = HF mice; end point body weight $p<0.0001$ for BL6, 129X1, DBA/2 and FVB/N; n = 6-8 for each strain and diet group.

Figure 2: Muscle (A) and Liver (B) triglyceride levels in low-fat (LF) and high-fat (HF) fed mice; white bars = LF mice, black bars = HF mice; † $p<0.01$, ‡ $p<0.001$; n = 6-8 for each strain and diet group.

Figure 3: Markers of mitochondrial oxidative metabolism in skeletal muscle. (A) Representative immunoblotting results on muscle oxidative proteins in low-fat (LF) and high-fat (HF) fed mice. Shown is n=2, but percentage differences underneath the corresponding lanes represent n=6-8 for each strain and diet group. Only significant ($p<0.05$) differences between the diet groups are shown. Complex I-V represent subunits of the complexes of the ETC chain. Skeletal actin in muscle was used as loading control and shows similar distribution between LF- and HF- groups in each strain. (B and C) citrate synthase and β-hydroxyacyl CoA dehydrogenase (βHAD) activity in low-fat (LF) and high-fat (HF) fed mice; white bars = LF mice, black bars = HF mice; * $p<0.05$, † $p<0.01$; n = 6-8 for each strain and diet group.

Figure 4: Markers of oxidative metabolism, lipid synthesis and lipid uptake in the liver. Representative immunoblotting results on oxidative and lipogenic enzymes and fatty acid transporters in low-fat (LF) and high-fat (HF) fed mice. Shown is n=2, but percentage differences underneath the corresponding lanes represent n=6-8 for each strain and diet group. Only significant ($p<0.05$) differences between the diet groups are shown. 14-3-3 was

used as loading control and shows similar distribution between LF- and HF- groups in each strain.

Figure 5: Inflammation in adipose tissue. Gene expression analysis of (A) F4/80, (B) CD68 and (C) CD11c+, (D) TNFα, (E) MCP-1 and (F) IL-6 in epididymal adipose tissue of low-fat (LF) and high-fat (HF) fed mice; white bars = LF mice, black bars = HF mice; * $p<0.05$, † $p<0.01$, ‡ $p<0.001$; n = 5 for each strain and diet group.

Figure 6: Markers of lipid peroxidative damage in muscle and liver. Lipid hydroperoxides (LOOH) (A and C) and TBARS (B and D) were measured in low-fat (LF) and high-fat (HF) fed mice as marker of oxidative stress; white bars = LF mice, black bars = HF mice; * $p<0.05$, † $p<0.01$; n = 6-8 for each strain and diet group.

Figures

Figure 1

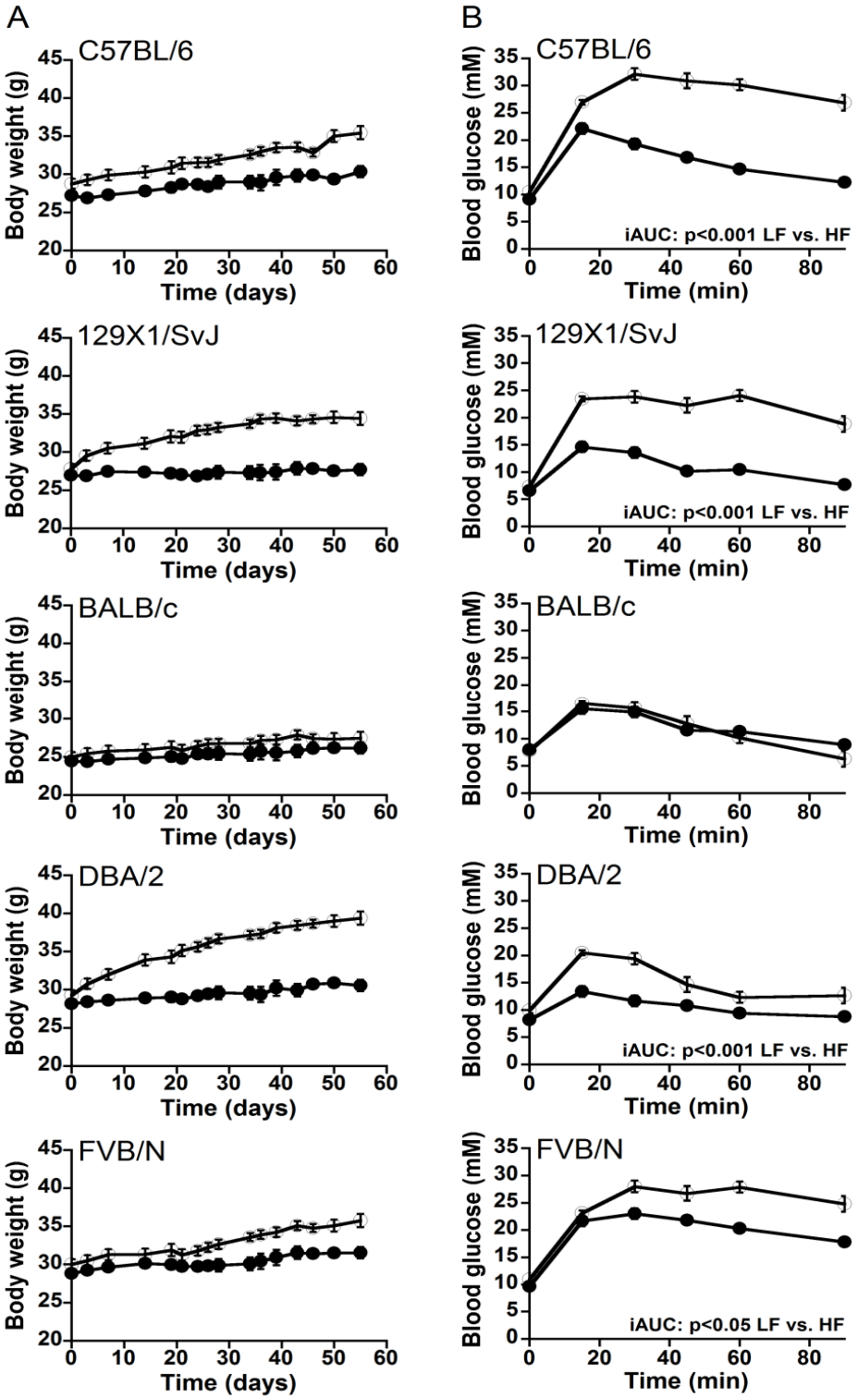

Figure 2

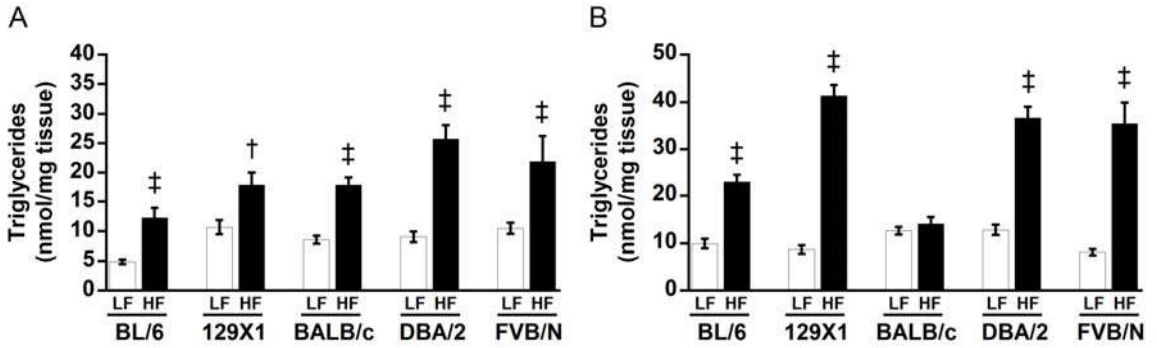

Figure 3

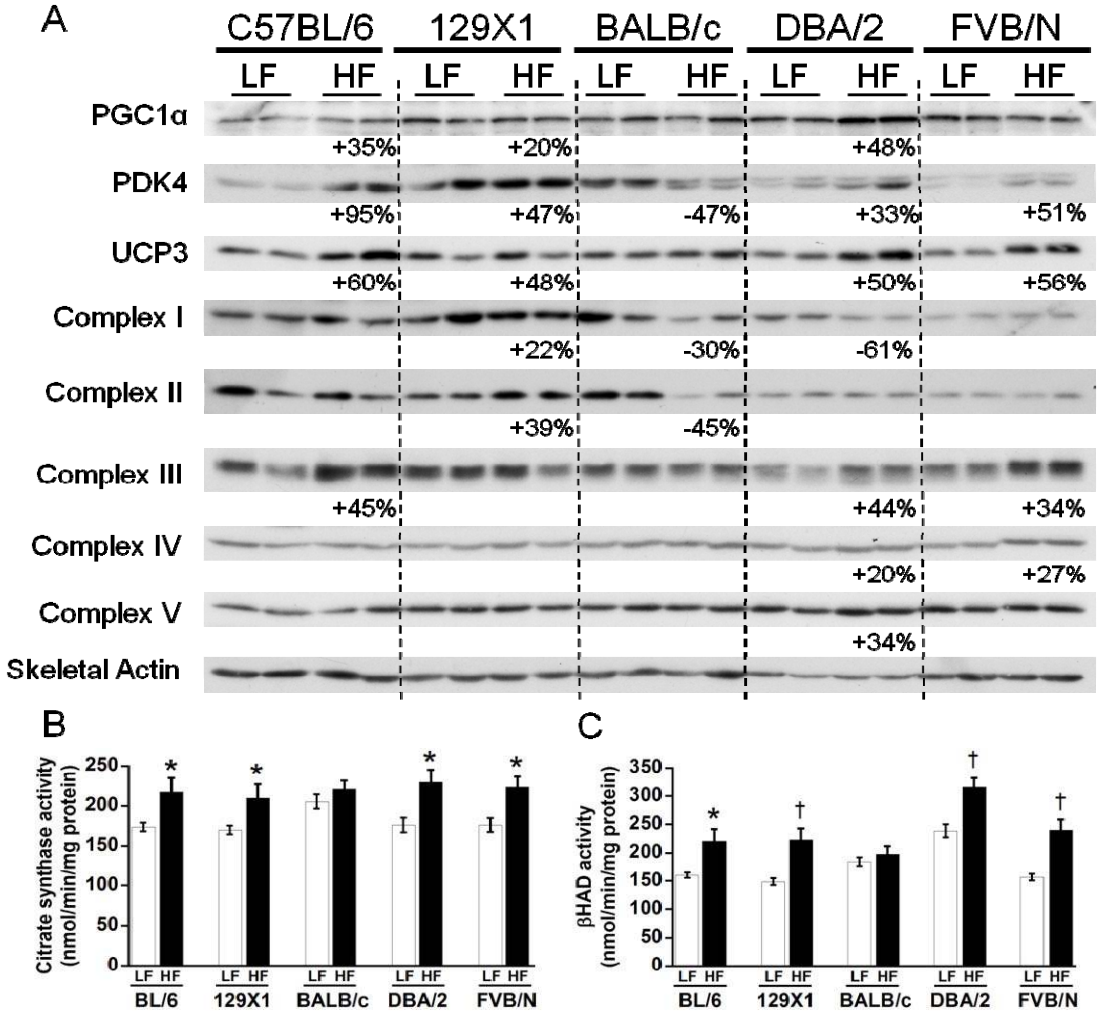

Figure 4

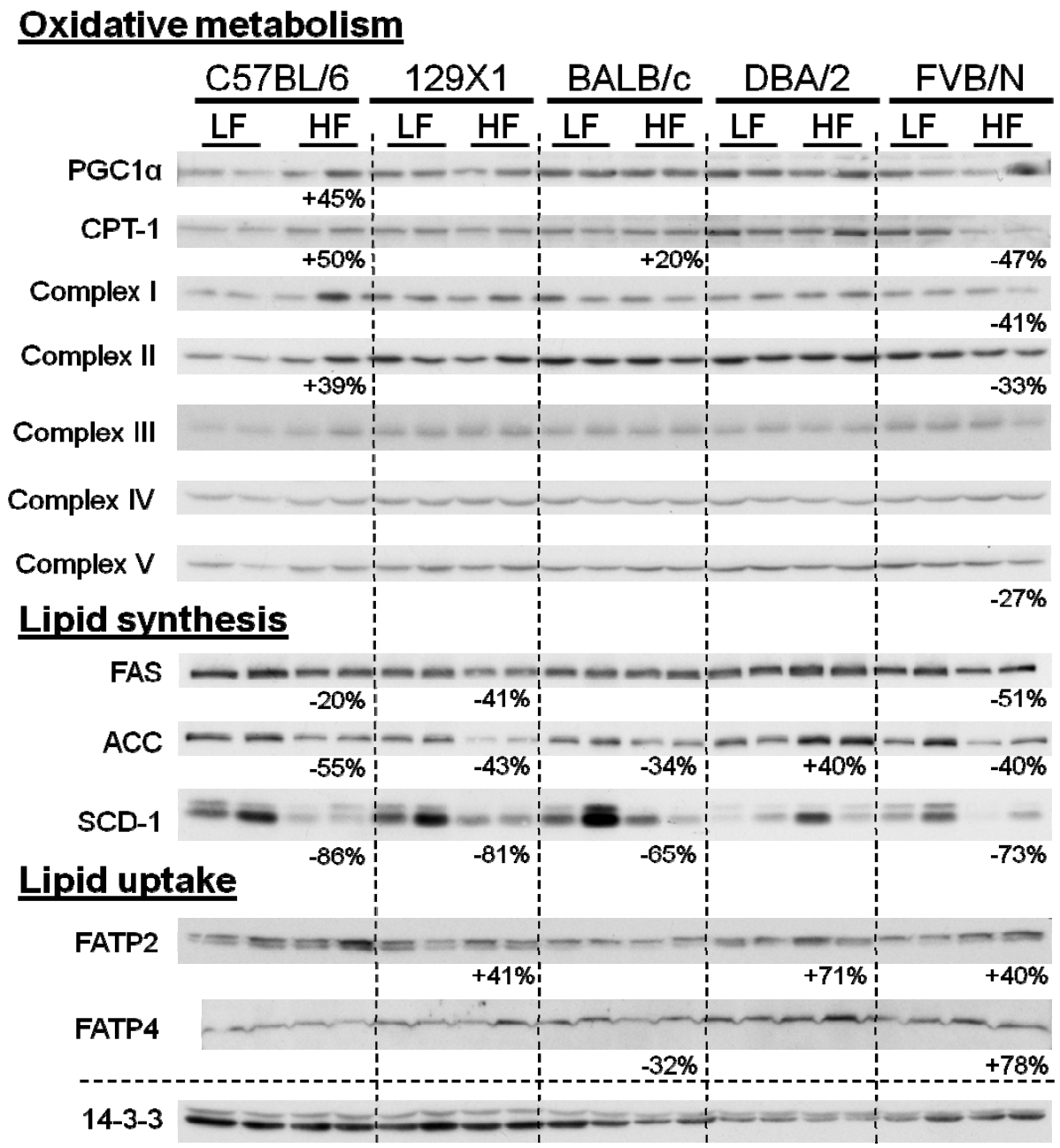
Oxidative metabolism
C57BL/6
129X1
BALB/c
DBA/2
FVB/N
LF
HF
PGC1α
+45%
CPT-1
+50%
+20%
-47%
Complex I
-41%
Complex II
+39%
-33%
Complex III
Complex IV
Complex V
-27%
Lipid synthesis
FAS
-20%
-41%
-51%
ACC
-55%
-43%
-34%
+40%
-40%
SCD-1
-86%
-81%
-65%
-73%
Lipid uptake
FATP2
+41%
+71%
+40%
FATP4
-32%
+78%
14-3-3

Figure 5

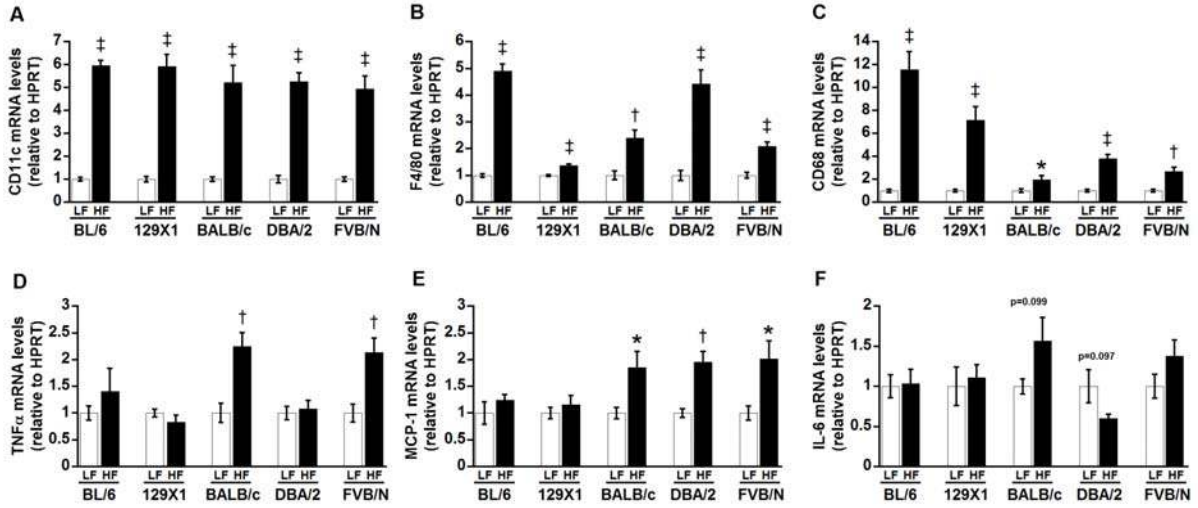

Figure 6